A SIMPLIFIED MODEL FOR THE FLOW IN A PROGRESSIVE CAVITY PUMP

Paulo A. S. Pessoa, pauloalison@msn.com
PPGEM - Graduate Program in Mechanical Engineering, Federal University of Rio Grande do Norte, CEP 59072-970- Natal - RN

Emilio E. Paladino, emilio@dem.ufrn.br
João A. de Lima, jalima@dem.ufrn.br
Department of Mechanical Engineering, Federal University of Rio Grande do Norte, CEP 59072-970- Natal - RN

Abstract. *The use of Progressing Cavity Pumps -PCPs- in downhole pumping applications in low deep wells is becoming more common replacing, in some cases, the traditional reciprocating pumps. Among the main advantages of this system the ability to pump heavy oils, produce large concentrations of sand, tolerate high percentages of free gas and high efficiency, can be quoted. The PCP system development, operation and control requires models able to predict flow rate for a given differential pressure, which has to be accurate and requires low CPU efforts in order to be an easy-to-use engineering tool or run on-line in a control loop. This work presents a simplified model for the flow in a Progressing Cavity Pump, based on mass balance within cavities and a simplification of momentum equations for fully developed flow. An adjustable parameter is required, but once this parameter is adjusted for a given pump geometry other operational conditions can be reproduced. Model is based on an approach already presented in literature, but a formal model development is presented and some improvements are introduced on friction factor calculation allowing the flow calculation of low viscosity fluids, which was not well succeeded in previous works.*

Keywords*: Pumps, PCP, simplified model, viscosity, roughness.*

1. INTRODUCTION

Progressing Cavity Pumps -PCPs- are becoming the preferred artificial lift system in low deep wells due to its several advantages as ability to pump heavy oils, produce large concentrations of sand and tolerate high percentages of free gas, among others. Although the concept has been proposed by Rene Moineau in 1930 (Moineau , 1930), first applications to oil production date from the 1970's. As a relatively new technology, at least in terms of application to oil industry, one of the main shortcomings is the lack of knowledge of the system, specifically, of the flow behavior, which would provide valuable information for system design, operation and control.

Together with the PCP system, Moineau (1930) proposed a simplified approach to characterize the flow within the device. The basic idea of this approach is to establish relations between differential pressure and flow rate by subtracting the counterflow leaked from seals, from the displaced flow rate. As this displaced flow rate depends only on pump geometry and kinematics, models calculate the leakage or "slippage"[1], and then the pumped flow rate, as function of the differential pressure. More recently, other works (Vetter and Paluchowski, 1997; Robello and Saveth, 1998) presented simplified models for predicting PCP performance which do not relate stator deformation with hydrodynamic phenomena inside the pump.

Although several works related to the PCP application and control in artificial lift systems were published, few references were encountered aiming the flow characterization within these devices. Robello & Saveth (1998) developed optimal relationships between the pitch and the diameter of the stator to achieve a maximum flow rate for multilobe pumps. This work is focused on pump geometrical parameters and their influence on displaced flow rate, but no mention is done to the slippage or to the influence of differential pressure on pumped flow rate. Olivet *et al.* (2002) performed an experimental study and obtained characteristic curves and instantaneous pressure profiles along metal to metal (rigid stator) pumps for single and two-phase flow conditions.

Gamboa *et al.* (2002) presented some attempts of flow modeling within a PCP using Computational Fluid Dynamics (CFD) with the aim of getting a better comprehension of the flow inside the pump but, attempts for the implementation of a three-dimensional model, including rotor motion, failed. Hence, authors concluded that numerical technique used for the flow modeling was inadequate for that purpose. Nevertheless, a model with these characteristics was successfully implemented in the context of this research project and is described in Paladino *et al.* (2009). Results from this model are used for the calibration of the simplified model presented in this work.

Gamboa *et al.* (2003) presented a simplified model for single phase flow considering the possibility of variable gap due to elastomeric stator deformation. The model is similar to presented in previous works, based on the aforementioned Moineau's approach, but the slippage is calculated considering the possibility of a variation of the clearance as function of differential pressure. In this way they were able to reproduce the characteristic non-linear behavior of volumetric flow versus differential pressure in a PCP with elastomeric stator. Gamboa *et al.* (2003) also proposed a slip model inside a single lobe PCP for single phase flow based on a previous model proposed by Vetter *et al.* (1993) and Vetter *et al.* (2000) for twin screw pumps.

[1] This term is commonly used in PCP and screw pumps terminology, as fluid is displaced axially through the pump, and counterflow "slips" over the displaced flow.

Another interesting model was presented in Andrade (2008) who solved the flow within a "developed" pump, i.e., the flow was solved between two plates, which local separation corresponds to the distance between rotor and stator, using an approach similar to the lubrication theory, where the inertial terms are neglected in transport equations. This approach presents good results for viscous fluids, but it is not suitable for low viscosity fluids where inertial terms become important and flow can eventually become turbulent.

This work presents the detailed development of a simplified flow model which can predict the operational curves of a PCP. Simplified models usually require some adjustable parameters. In this case, adjustable parameters are reduced to an only geometrical one, which is adjusted using results form a detailed 3D CFD model, developed in the context of this research. This information is of fundamental importance in terms of system design and operation control. Furthermore, as a simple model, CPU requirements are minimum, which would make it able to run on-line in a control loops.

Although the CFD model can provide detailed information about the pump performance for different geometrical parameters and operational conditions, the simplified model presented, is able to calculate pump performance with minimum CPU requirements, which makes it able to run on-line in a control loop or develop fast engineering projects.

The basic idea of the model is to establish relations between differential pressure between cavities and flow rate across sealing regions by considering a Poiseuille flow in order to predict the internal slip, which is subtracted from the displaced volumetric flow rate. Although the general framework of the model is based on already published works (Vetter *et al.* (1997), Gamboa *et al.* (2003)), a formal development of the model equations based on mass and momentum balances within cavities is presented and some aspects regarding the friction factors, which have strong influence on pump performance, are investigated.

1.1. PCP operation principle

This section aims to describe briefly the operational principle of a PCP, in order to understand the shortcomings of the flow modeling within it. However, a detailed explanation of PCPs design and operation is beyond the scope of this paper and can be encountered, for instance, in Nelik & Brennan (2005), ISO (2008) and other references.

The PCP is a rotary positive displacement pump, also known as eccentric screw pumps, it is constituted by two elements, rotor and stator.

The stator can be constituted of steel or elastomer and its internal surface is the envelope of an N steps helical without eccentricity. The rotor is made of metal and its surface is the envelope of an N-1 steps helical with eccentricity and step equal to half the stator's step. In the Figure 1 can identify these two components and their position in the pump.

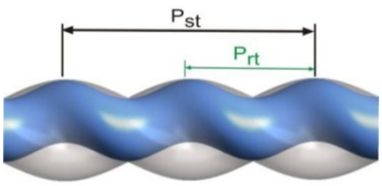

Figure 1. Stator and rotor step

When the rotor is inserted inside the stator, a series of cavities isolated from one another by seal lines is formed, as shown in Fig. 2. Due to the eccentric motion of the rotor within the stator, the fluid within cavities is displaced axially from the pump suction port to the discharge (high pressure) port.

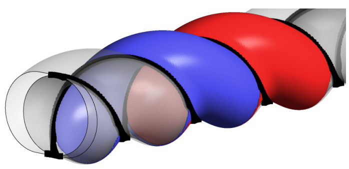

Figure 2. PCP cavities and seal lines

The distance between the stator and rotor, which can be calculated as,

$$w = \frac{d_{ROTOR} - d_{STATOR}}{2} \qquad (1)$$

The PCP can operate with interference or clearance between rotor and stator, depending if w is positive or negative. Both situations are depicted in Fig. 3. For the case operating with interference a deformable stator is needed and is manufactured using an elastomeric material. In this case, the stator deformation due to the fluid pressure has to be computed for calculating the pumped flow rate, due to the strong influence of the clearance on the slippage.

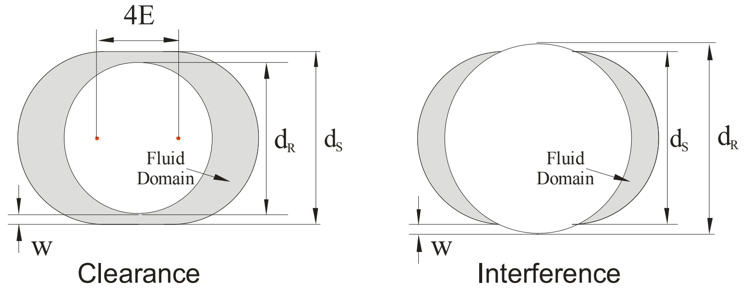

Figure 3. Relationship between rotor and stator diameter

Four main geometrical parameters characterize a PCP: the rotor diameter, eccentricity, interference and stator pitch. Since the first three determine the area of a cross section of the pump, while the last determines the volume displaced. The theoretical displaced volume in each rotation, can be calculated for the case of clearance and interference, respectively as,

$$V_{th} = \left[4 \cdot E \cdot d_R - 8 \cdot E \cdot w - \pi \left(w \cdot d_R - w^2 \right) \right] \cdot P_{ST} \ , \quad w < 0$$

$$V_{th} = \left[4 \cdot E \cdot d_R - 8 \cdot E \cdot w - \pi \left(w \cdot d_R + w^2 \right) + \frac{{d_R}^2}{2} \cdot \arcsin\left(\frac{2}{d_R} \sqrt{w \cdot d_R - w^2} \right) - 2\left(\frac{d_R}{2} - w^2 \right) \cdot \sqrt{w \cdot d_R - w^2} \right] \cdot P_{ST} \ , \quad w > 0 \tag{2}$$

The flow rate displaced is calculated multiplying the volumes given in Eq. (2) by the rotation velocity and represents the maximum flow rate that can be pumped (for Δp=0, i. e. zero slippage). As stated, the actual pumped flow rate can be determined by subtracting the slip, from the displaced flow rate.

The slippage is function of pump geometry, fluid viscosity and differential pressure along the pump. Figure 4 shows schematically the typical shape of performance curves for elastomeric and metallic stator. For the case of elastomeric stator, the pump operates with interference between rotor and stator at zero pressure drop and, for operation at low pressures, the cavities are maintained enclosed and the pumped flow rate is equal to the displaced flow rate. However, as the stator is deformable, the deformation will be increased with internal pressure and so the slippage between cavities. When the deformation exceeds the interference, the slippage increases more significantly with pressure drop. For the metallic stator case, the clearance between rotor and stator which is constant. Then, for high viscosity fluids the flow along the sealing regions is laminar, and slippage varies linearly with pressure drop as for turbulent flow case, the slippage will be proportional to some power, n<1, of pressure drop.

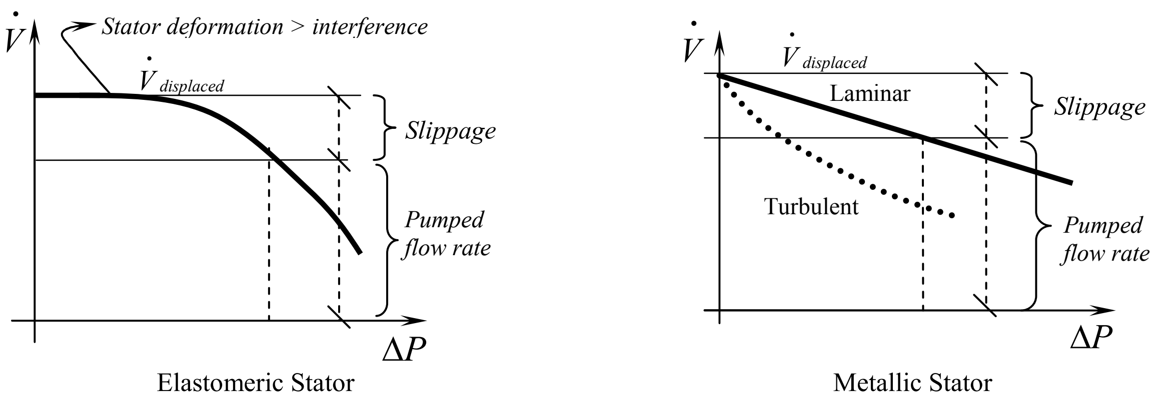

Figure 4. Expected characteristic curves for metallic (a) and elastomeric (b) stator PCPs

2. FLOW MODEL

Before the development of the flow model, the general idea of the approach proposed by Moineau (1930) for calculating the internal slippage in a PCP is presented. This approach is based on the consideration of a Hagen-Poiseuille flow along the sealing regions.

Assuming constant value for the clearance along the pump, the slip flow can be calculated considering the flow between parallel plates, separated by a distance equal to the clearance.

Considering a channel between cavities, i.e., across the sealing lines, which main geometric parameters are shown in Fig. 5, the pressure drop can be calculated as

$$\Delta p = f\,\frac{\rho}{2}\overline{U}^2\,\frac{L}{D_H} \tag{3}$$

where f is the friction factor and D_H is the hydraulic diameter, defined as four times the cross sectional area over the perimeter.

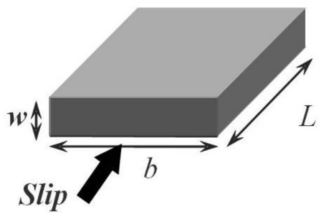

Figure 5. Characteristic dimensions in a rectangular channel

Recalling that the mean velocity across the channel corresponds to the volume flow rate divided by the cross sectional area, the pressure drop can be calculated as

$$\Delta p = f\,\frac{\rho L}{4b^2w^3}S^2 \tag{4}$$

In equation above, it was considered that $w \ll b$ when calculating the hydraulic diameter. For laminar flow, the friction factor can be calculated as

$$f = \frac{C}{\mathrm{Re}} \quad where \quad \mathrm{Re} = \frac{2\rho S}{\mu b} \tag{5}$$

where S is the slip flow through the seal lines. The generic constant C was used because, as this analysis does not intend to be quantitative, but just qualitative and the channel geometry is not, *a priori*, known. At this point, it is important to say that one of the strongest hypotheses in these approaches is the simplification of the channel geometry as the actual sealing is produced in a convergent-divergent geometry.

Following previous equations, the slip can be calculated as,

$$S = \frac{8}{C}\frac{bw^3\Delta p}{\mu L} \tag{6}$$

This slip flow can be subtracted from the theoretical volumetric flow rate, which depend just on geometrical parameters and rotation, in order to obtain the pumped flow rate as function of the pressure drop. Then, from this simple analysis the pump performance can be related, at least qualitatively, to the main pump geometric parameters and fluid properties.

From Equation (6) obtained from a very simple analysis some issues can be highlighted, which are also observed in experimental results:

- For laminar flow, which has been assumed for this analysis, the slip depends linearly on the pressure difference across the pump (Δp) and the fluid viscosity (μ) has a inverse linear influence.
- The clearance (w) appears elevated to the cube, which means it has a strong influence on the volumetric efficiency.
- The length L has also a inverse linear influence on the flow rate. In practice, this parameter can be increased by increasing the number of pump stages. This is equivalent to put more "sealing channels" in serial augmenting the resistance to the slippage.

In addition, it is observed in Eq. (6) that fluid density does not influence the slippage. This is because fully developed laminar flow has been assumed along the seal region. This means that the flow along the sealing region is established owing to a balance between pressure and viscosity forces, neglecting the inertia. Then, the rotation velocity has no influence either.

In order to turn this analysis quantitative, the assumed channel dimensions have to be related to the pump geometric parameters. We recall that in the real geometry, the "channel" considered in preceding analysis is actually a convergent-divergent section, and the channel length, L is actually an equivalent one, which provides the same resistance to flow as a constant section channel. This is one of the main difficulties of this approach, and this parameter should be adjusted experimentally or from more realistic models, as done in this work.

2.1. Model description

Based on an approach similar to the described in the previous section, Gamboa *et al.* (2003) presented a more detailed model, which calculates the slip between cavities as the sum of two components; the flow "along" the pump and the flow "across" it. These components of the slip are shown schematically in the Fig. 6.

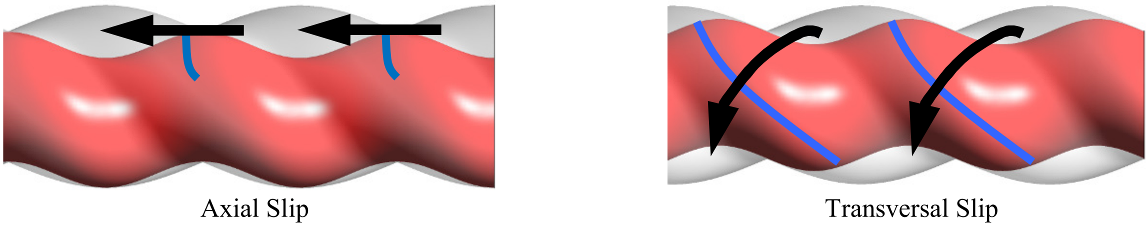

Figure 6. Slip regions between cavities in a PCP and seal regions (blue lines)

The slippage calculation is split in two components, as channel characteristic dimensions are different for each component.

The channel width is considered equal to the length of the seal line. For the case of the axial channel, the width can be calculated as half of the circumference length, as depicted in Fig. 7.

$$b_L = \pi \frac{d_S}{2} \tag{7}$$

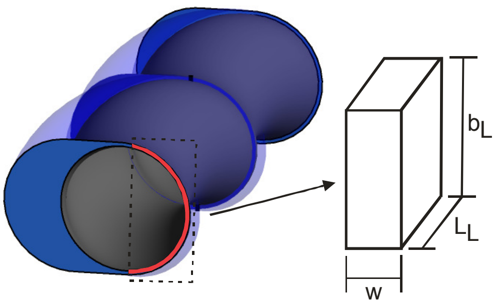

Figure 7 –Axial channel width

For the case of transversal channel, the width corresponds to the distance between points A and B which is the length of the seal line between two cavities, showed in Fig 8.

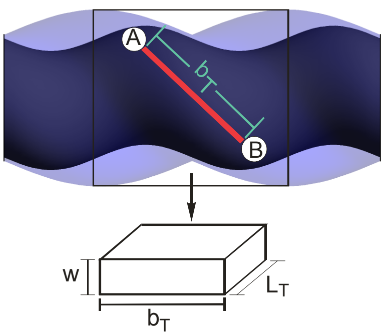

Figure 8 – Transversal channel width

This distance can be calculated using the parametric equations for the rotor surface (Eq. (8)) taking a differential length of a seal line (which coordinates are obtained making $\alpha = 0$ or $\alpha = \pi$ in Eq. (8)) and integrating the over a half of stator pitch, Eq. (9).

$$X_R(\alpha,\theta_S) = \frac{d_R}{2}\cdot Sin(\alpha) - e\cdot Sin(2\cdot\theta_S)\ ,\quad Y_R(\alpha,\theta_S) = \frac{d_R}{2}\cdot Cos(\alpha) + e\cdot Cos(2\cdot\theta_S)\ ,\quad Z_R(\alpha,\theta_S) = \frac{2\cdot\theta_S}{4\cdot\pi}\cdot P_S \tag{8}$$

$$b_T = \int_{\theta_S=0}^{\theta_S=\pi} \sqrt{\left(\frac{dX_R(\alpha,\theta_S)}{d\theta_S}\right)^2 + \left(\frac{dY_R(\alpha,\theta_S)}{d\theta_S}\right)^2 + \left(\frac{dZ_R(\alpha,\theta_S)}{d\theta_S}\right)^2}\, d\theta_S \tag{9}$$

Once having the characteristic geometrical parameters of the channels, a mass balance is performed for each cavity in order to obtain the pressure within cavities.

Figure 9 depicts the conceptual approach used in this model, and how pump geometry is simplified. The resulting geometry consist in cavities with constant pressure within them, and constant cross section channels representing the sealing regions

In order to generalize the model for any number of cavities, it is assumed, according to Gamboa (2000), that the transversal slip leaks from cavity *i* to cavity *i-1* and other axial slip flows from cavity *i* to cavity *i-2*,. Then a mass balance in each cavity is performed summing these components.

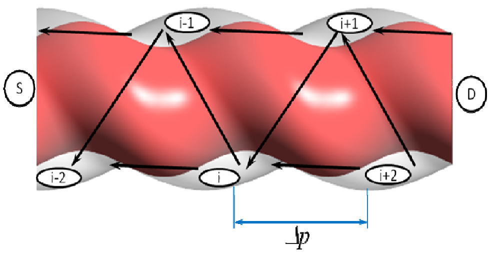

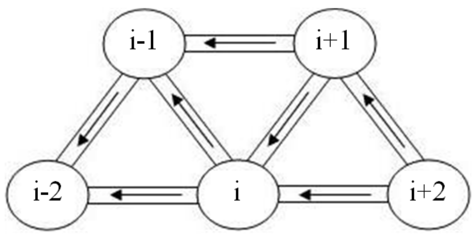

Figure 9. Slip scheme within the PCP

Following Vetter *et al*. (1993 e 2000) proposed approaches for twin screw pumps, Gamboa *et al*. (2003), suggested to include into the slippage calculation a component due to the rotor motion as a Couette flow. Depending on the cavity position, this component can be co- or countercurrent with the flow due to pressure difference between cavities ("Poiseuille" component). Nevertheless it can be demonstrated that this "Couette" component of the slippage is small, when compared with slippage due to pressure differences between cavities, and was neglected in this model.

Equation (2) represents the momentum conservation equation for fully developed flow between parallel plates resulting from a balance between pressure and viscous forces. For the case of laminar flow, this equation results in eq. (6) where pressure drop varies linearly with slippage, as friction factor is inversely proportional to the volumetric flow rate.

As proposed in the present model, it is considered that slippage has two components; axial and transversal. Then, rewriting eq. (5) in terms of geometrical parameters referent to transversal and axial, we have:

$$\begin{aligned} S_T &= \frac{1}{R_T}\Delta P \quad \text{where} \quad R_T = \frac{C\cdot\mu\cdot L_T}{8\cdot b_T\cdot w^3} \\ S_L &= \frac{1}{R_L}\Delta P \quad \text{where} \quad R_L = \frac{C\cdot\mu\cdot L_L}{8\cdot b_L\cdot w^3} \end{aligned} \tag{10}$$

where R_T and R_L represent the transversal and axial "flow resistances" of seal regions.

Taking the mass conservation equation for cavity *i* in scheme showed in Figure 8,

$$\sum_{Cavities} S = 0 \tag{11}$$

and using eqs. (10), we have

$$\sum_{Cavities} S = \frac{\Delta P_{i-2,i}}{R_{Li-2,i}} + \frac{\Delta P_{i-1,i}}{R_{Ti-1,i}} - \frac{\Delta P_{i,i+1}}{R_{Ti,i+1}} - \frac{\Delta P_{i,i+2}}{R_{Li,i+2}} = 0 \tag{12}$$

Rearranging, we get a liner system which unknowns are the pressures in each cavity

$$\frac{P_{i-2} - P_i}{R_{Li-2,i}} + \frac{P_{i-1} - P_i}{R_{Ti-1,i}} - \frac{P_i - P_{i+1}}{R_{Ti,i+1}} - \frac{P_i - P_{i+2}}{R_{Li,i+2}} = 0 \tag{13}$$

Equation (14) can be assembled in a pentadiagonal linear system to calculate the pressures in each cavity, as

$$\begin{bmatrix} \ddots & \ddots & \ddots & \ddots & \ddots & \ddots & 0 \\ \ddots & A_{Pi-2} & \frac{1}{R_{Ti-2,i-1}} & \frac{1}{R_{Li-2,i}} & 0 & 0 & 0 \\ \ddots & \frac{1}{R_{Ti-2,i-1}} & A_{Pi-1} & \frac{1}{R_{Ti-1,i}} & \frac{1}{R_{Li-1,i+1}} & 0 & 0 \\ 0 & \frac{1}{R_{Li-2,i}} & \frac{1}{R_{Ti-1,i}} & A_{Pi} & \frac{1}{R_{Ti,i+1}} & \frac{1}{R_{Li,i+2}} & 0 \\ 0 & 0 & \frac{1}{R_{Li-1,i+1}} & \frac{1}{R_{Ti,i+1}} & A_{Pi+1} & \frac{1}{R_{Ti+1,i+2}} & \ddots \\ 0 & 0 & 0 & \frac{1}{R_{Li,i+2}} & \frac{1}{R_{Ti+1,i+2}} & A_{Pi+2} & \ddots \\ 0 & \ddots & \ddots & \ddots & \ddots & \ddots & \ddots \end{bmatrix} \begin{bmatrix} \vdots \\ P_{i-2} \\ P_{i-1} \\ P_i \\ P_{i+1} \\ P_{i+2} \\ \vdots \end{bmatrix} = \begin{bmatrix} \vdots \\ b_{i-2} \\ b_{i-1} \\ b_i \\ b_{i+1} \\ b_{i+2} \\ \vdots \end{bmatrix} \tag{14}$$

where

$$A_{Pi} = \frac{1}{R_{Li-2,i}} + \frac{1}{R_{Ti-1,i}} + \frac{1}{R_{Ti,i+1}} + \frac{1}{R_{Li,i+2}} = 0 \tag{15}$$

Note that the momentum conservation equations, simplified for fully developed flow, were substituted into the mass conservation equation resulting in a linear system for pressures. The pressures obtained are such that the resulting flow rates from momentum equation satisfy the mass conservation. This approach is similar to what is usually done in numerical solution of incompressible (or weak compressible) flows to calculate pressure field from mass conservation equation (see, for instance, Maliska (2004) or Ferziger & Peric (2001)). Obviously, this case is much simpler, as momentum equation does not include inertial (non linear) terms due to the fully developed flow hypothesis.

When flow along the seal regions becomes turbulent, equation (3) is used, considering the friction factor, f as function of channel Reynolds number. Then, slip flow rates for transversal and axial channels are given by,

$$S_T = \frac{1}{R_T}\Delta P \quad \text{where} \quad R_T = \frac{f_T \cdot \rho \cdot L_T \cdot S_T^*}{4 \cdot {b_T}^2 \cdot w^3} \tag{16}$$

$$S_L = \frac{1}{R_L}\Delta P \quad \text{where} \quad R_L = \frac{f_L \cdot \rho \cdot L_L \cdot S_L^*}{4 \cdot {b_L}^2 \cdot w^3} \tag{17}$$

Note that, due to the non linear dependence of pressure drop with slip flow for turbulent flows, the system needs to be solved iteratively. Here, as the resulting system is simple and converges quickly, a simple linearization was used, just splitting $S^2 = S \cdot S^*$ ("*" mean the value from previous iteration), instead of Newton or Newton-Raphson or other usual methods for solving non linear equations.

The friction factor was calculated using the Colebrook equation.

$$f = \left[-2 \cdot Log_{10} \left(\frac{e/_{D_H}}{3,7} + \frac{2,51}{\mathrm{Re}\sqrt{f}} \right) \right]^{-2} \tag{18}$$

Once the linear system is solved using Gauss-Seidel method, the pressure within each cavity is known and the slippage for each internal channel can be calculated. The total slippage is calculated as the sum the transversal as longitudinal slippages.

$$S = \frac{\Delta P_{i-2,i}}{R_{Li-2,i}} + \frac{\Delta P_{i-1,i}}{R_{Ti-1,i}} \quad or \quad S = -\frac{\Delta P_{i,i+1}}{R_{Ti,i+1}} - \frac{\Delta P_{i,i+2}}{R_{Li,i+2}} \tag{19}$$

For the case of rigid (steel) stator pump, the clearance along the pump is constant, and the slippage between any two cavities will be the same. Nevertheless, it is important to mention, that the present model is applicable to deformable stator pumps, since a relation between the clearance variation, due to the stator deformation, and pressure can be introduced, as the pressures are calculated independently for each cavity. In this paper the model validation is done for a rigid stator pump.

2.2. MODEL CALIBRATION

The calibration parameters L_L and L_T were obtained using results from a detailed CFD model which solves the transient Navier Stokes equations within the PCP, considering the real geometry and the rotor motion. Details of the implementation of this model can be encountered in Paladino *et al.* (2009). The simplified model can be also adjusted through experimental data, nevertheless, experimentation is expensive and, sometimes, real operational conditions, as downhole pressures and temperatures are difficult (or impossible) to reproduce in laboratory tests, but can easily studied though a computational model.

As stated, L_L and L_T represent the lengths considered for axial and transversal channels, which results on the same pressure drop of the sealing region. The "channel" considered in this model represent, in the actual geometry, a convergent-divergent channel. The concept is depicted in Fig. 10. As L_L and L_T represent similar concepts, they were made equal, resulting in one adjustable parameter for the model, $L_L = L_T = L$.

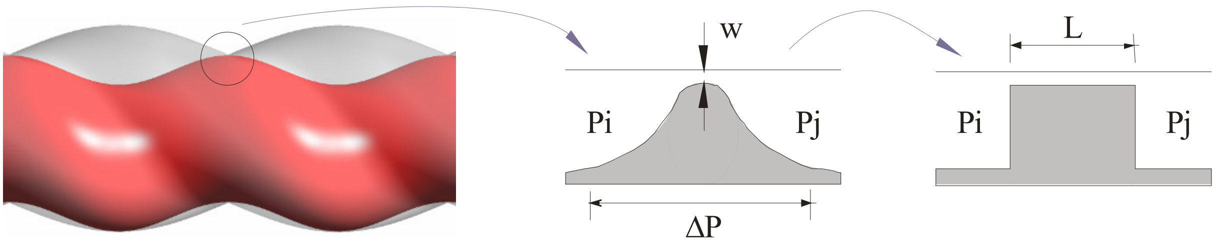

Figure 10. Approach slippage channel length

The parameter L is determined by "trial and error" in such way that the simplified model gives the same mass flow rate of 3D model for a given operational condition.

At this point, one could ask: why to do all this analysis, including friction factor calculations, instead of simply adjust flow resistance which provides the same pressure drop of 3D model or experiments? The answer is simple: once the parameter is adjusted for a given pump geometry for **one** operational condition and **one** fluid, the curves for other operational conditions and fluid properties are determined using the same value for L, as will be seen in results section. Then it is concluded that this parameter depends only on pump geometry.

3. RESULTS

This section presents operational curves of flow rate versus differential pressure, for a pump used in Gamboa *et al.* (2002) and Olivet *et al.* (2002) experimental works for single-phase flow. Geometrical parameters for this pump are presented in the Table 1.

Table 1. Geometrical parameters of the PCP used in Gamboa *et al.* (2002)

Eccentricity – **E**	**4,039 mm**
Rotor Diameter– $\mathbf{d_R}$	**39,878 mm**
Stator Diameter – $\mathbf{d_S}$	**40,248 mm**
Clearance	**0,185 mm**
Stator Pitch	**119,990 mm**
Number of Stator Pitches	**3**

Three fluids were considered for model validation; a medium viscosity oil, a high viscosity oil and water. The properties of these fluids are presented in Table 2

Table 2. Fluids Properties of the PCP used in Gamboa *et al*. (2002)

Properties	Oil		Water
Specific density – ρ	**868 kg/m³**	**885 kg/m³**	**997 kg/m³**
Viscosity– μ	**42 cP**	**481 cP**	**1 cP**

A case with 42 cP oil, Δp=20 and rotation velocity of 300 rpm was used for model calibration. The value of *L* which provides the same mass flow calculated by the 3D model, for these operational condition and fluid properties is: ***L*=1.65mm**. Results were validated for rotation velocities of 100, 200, 300 and 400 rpm for oil flow and 300 and 400 rpm for water flow.

Results for volumetric flow rate versus differential pressure are showed in Fig. 11, compared with experimental results from Gamboa *et al.* (2002) and Gamboa *et al.* (2003).

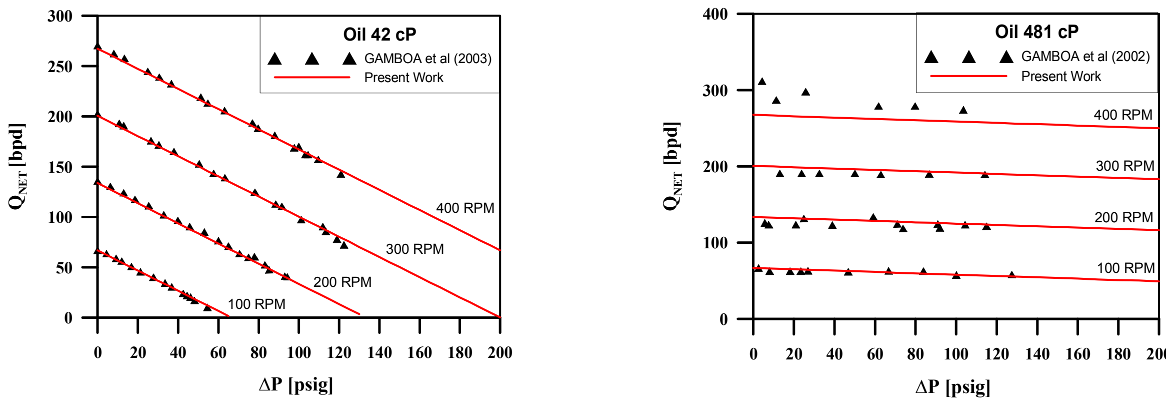

Figure 11. Flow rate versus differential pressure, for different rotation velocities, compared with experimental results for different oil viscosities. (a) 42 cP and (b) 481 cP

It can be seen in Fig. (11) that curves for high viscosity fluids present a linear behavior as flow is laminar and then, pressure drop along sealing regions varies linearly with slip. In this case surface roughness has not any influence on friction factor.

For the case of water flow, the results of flow rate versus differential pressure were obtained considering different material roughness, and can be seen in Fig. 12 compared with experimental results from Gamboa *et al.* (2003).

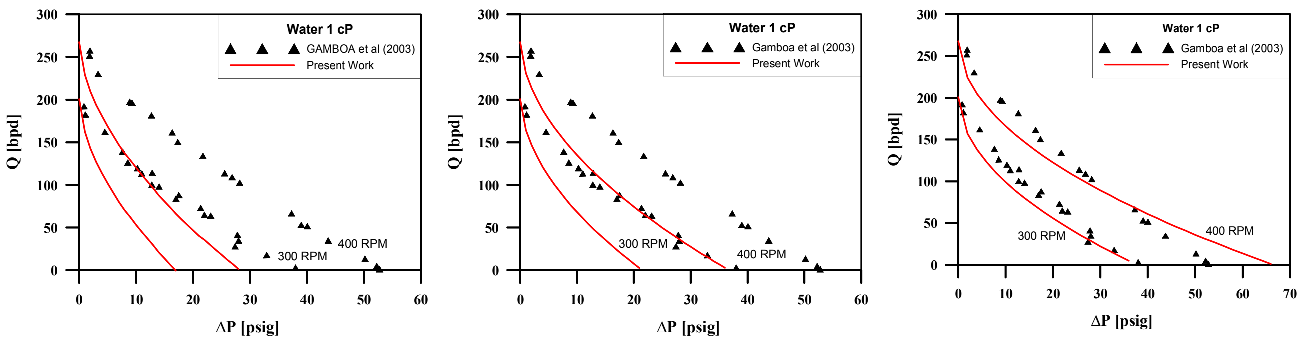

(a) Smooth (b) Stainless steel (c) Stretched steel

Figure 12. Flow rate versus differential pressure, for water (1 cP) and different rotation velocities and roughness, compared with experimental results from Gamboa *et al.* (2003). (a) Smooth wall, (b) Stainless steel (roughness = 0.002mm) and (c) Stretched steel (roughness = 0,015mm)

Gamboa *et al.* (2003) attempted to reproduce the water flow rate curves using a model similar to the hereby presented, but results severely under-predicted experimental values, i.e., slippage was over predicted. In that work, the friction factor was calculated trough a simplified model which does not considers the material surface roughness. The Nikuradse's approach ($f = 0.322/Re^{0.25}$) for friction factor for smooth pipe, was used.

Results in Fig. 12 show that roughness has an important influence on calculated flow rate for low viscosity fluids. Then, although further adjustment could be necessary for the case of occurrence of turbulent flow at seal lines, the main outcome from this analysis is that roughness values has a strong influence on model results and should be taken into account for friction factor calculation.

4. CONCLUSIONS

A simplified model for the flow in a PCP was successfully implemented which is able to predict flow rate for a given differential pressure, with almost negligible CPU requirement. This make the simplified model suitable to run on-line in control loops for PCP systems and can become and engineering tool for quick calculations.

Predictions for low viscosity fluids, where flow along seal lines can become turbulent, require the consideration of material surface roughness in the Colebrook's friction factor equation. This could maybe explain why model presented by Gamboa et al. (2003) was unable to reproduce experimental values for water flow.

As model considers the possibility of variable clearances along the pump, it can be extended for elastomeric (deformable) stator. This is object of current research.

5. ACKNOWLEDGEMENTS

Authors are grateful to CENPES, UN-RNCE/PETROBRAS and PRH 14-ANP for the financial support of the present research.

6. REFERENCES

Andrade, S. F., 2008, "Modelo Assintótico Para Escoamento Monofásico Em Bomba De Cavidade Progressiva , Pontificia Universidade Catoloca do Rio de Janeiro - PUC-Rio (in Portuguese).

Ferziger, J. H. & Peric, M., 2001. Computational Methods for Fluid Dynamics, Springer-Verlag Telos, 3 Edição.

Gamboa, J., Olivet, A., González, P. and Iglesias, J., 2002. "Understanding the Performance of a Progressive Cavity Pump with a Metallic Stator", Proceedings of the 20th International Pump Users Symposium.

Gamboa, J., Olivet, A. and Espin, S., 2003, "New Approach for Modeling Progressing Cavity Pumps Performance", SPE 84137. Paper presented at the SPE Annual Technical Conference and Exhibition. Denver, Colorado, 5-8, USA.

ISO, 2008. Downhole Equipment for Petroleum and Natural Gas Industries - Progressing Cavity Pump Systems for Artificial Lift.

Maliska, C. R., 2004, "Transferência De Calor e Mecânica Dos Fluidos Computacional", (*in Portuguese*), LTC Editora, 2ª Edição.

Moineau, R., 1930, "A new Capsulism", Doctoral Thesis, The University of Paris.

Nelik, L. and Brennan, J., 2005, "Progressing Cavity Pumps, Downhole Pumps and Mudmotors", Gulf Publish Company, Houston, Texas, USA.

Olivet, A., Gamboa, J. and Kenyery, F., 2002, "Experimental Study of Two-Phase Pumping in a Progressing Cavity Pump Metal to Metal", SPE 77730. Paper presented at the SPE Annual Technical Conference and Exhibition, San Antonio, Texas, 29 September-2 October, USA.

Robello, G. and Saveth, K., 1998, "Progressing Cavity Pump (PCP): New Performance Equations for Optimal Design", Paper presented at the 1998 SPE Permian Basin Oil and Gas Recovery Conference, Midland, Texas, US.

Vetter, G. and Wincek, M., 1993, "Performance Prediction of Twin Screw Pumps for Two-Phase Gas/Liquid Flow, pumping Machinery", Edited by Paul Cooper, ASME, FED Vol. 154.

Vetter, G. and Paluchowski, D., 1997, "Modeling of NPSHR For Progressing Cavity Pumps", ASME Fluids Engineering Division Summer Meeting.

Vetter, G., Wirth, W. and Pregler, S., 2000, "Multiphase Pumping with Twin-Screw Pumps-Understand and Model Hydrodynamics and Hydroabrasive Wear", Proceedings of 17th International Pump Users Symposium.

7. RESPONSIBILITY NOTICE